Queueing analysis of ultra-wideband medium access control protocol with finite buffer

Mohamed Ali Ahmed

College of Community,
University of Hail,
KSA, Saudi Arabia
Email: ma.ahmed@uoh.edu.sa
and
Faculty of Science,
Suez Canal University, Egypt

Hassan Al-Mahdi*

Faculty of Computer and Informatics,
Suez Canal University, Egypt
Email: hassanwesf@yahoo.com
*Corresponding author

Abstract: Ultra-wideband (UWB) communication has recently emerged as a technology that offers high data rate services for future wireless personal area networks. Due to its high bandwidth, it is substantial effort to design medium access control (MAC) protocols that perfectly utilise the available shared bandwidth offered by UWB technology. This paper introduces an extensive 4-dimensional finite Markov chain queueing model to investigate the performance of a multi-band protocol that was proposed in literature in terms of system occupancy, waiting time, throughput, packet loss and blocking probabilities. Our motivation is to precisely estimate packets collision probability due to randomly selection of receivers or bands. Besides introducing the finite buffer, our queuing model reflects the system behaviour in-depth. Next, we validate the obtained analytic results using discrete-event simulation. Finally, we introduce an outline of a proposal to eliminate the randomness of selecting receivers and bands.

Keywords: ultra-wideband; UWB; queueing network; performance evaluation; medium access control; MAC; ad hoc networks; Markov chain; device discovery; ad hoc networks.

Reference to this paper should be made as follows: Ali Ahmed, M. and Al-Mahdi, H. (2019) 'Queueing analysis of ultra-wideband medium access control protocol with finite buffer', *Int. J. Ultra Wideband Communications and Systems*, Vol. 4, No. 1, pp.1–15.

Biographical notes: Mohamed Ali Ahmed received his BSc in Scientific Computations from the Faculty of Science, Suez Canal University, Egypt in 1994, his MSc degree in Computer Sciences in 2001, and his PhD degree in 2006 in Computer Science from the same university. His current research interests include network performance analysis and design of Mac protocols over broadband and ultra-wide band wireless networks.

Hassan Al-Mahdi received his BSc in Computing Science, MSc in Computer Science and PHD in Wireless Networks from the Faculty of Science, Suez Canal University, Egypt in 1994, 2001 and 2005, respectively. He is a Professor of Computer Networks at the Department of Computer Science, Faculty of Computer and Informatics Suez Canal University, Ismailia, Egypt. His research focuses on ad hoc networks, mobile cellular communications, cognitive radio networks and the performance evaluation of computer networks. He has many international papers mostly in the area of data communication and performance evaluation.

1 Introduction

The tremendous grow of advanced electronic devices storing data requires establishing wireless personal area networks (WPANs) to send data between those devices. Large data sizes saved in those devices require a fast technology to transmit those data with speed faster than Bluetooth or WiFi. Ultra-wideband (UWB) technology is a suitable candidate designed for WPANs, wireless sensor networks, wireless USB and hard disks. On the other hand, due to the great advances in both hardware and applications, large data sizes are generated. For example, new digital cameras create images and videos with high quality. So, it is important to store data packets of nodes losing the

contention in some suitable storage space. Attaching suitable buffers to devices is an important goal to reduce packet loss due to possible packet collisions.

UWB technologies have a great attention because of their large bandwidth (BW) and low power emission, which are suited to in-door, high-speed multimedia communications (Broustis et al., 2007; Zin and Hope, 2010; Liu et al., 2009). UWB is typically addressed and defined as a signal or system that either has a large relative BW exceeds 20% of its centre frequency or a large absolute BW of greater than 500 MHz (Zhuang et al., 2003; Shen et al., 2005; Lu et al., 2005a). Due to the significant BW of UWB, many sources can share the available BW to send data to various destinations simultaneously. Therefore, an exclusive care is needed to avoid data collisions on one side, and control data transmission simultaneously both in single band and multi-band UWB on the other side. Since controlling medium access sharing of UWB is a necessary objective, medium access control (MAC) protocols in UWB communication have got much attention within both research and industry when compared with traditional narrowband systems (Viswanathan and Ravi, 2005; Jiang and Zhuang, 2007; Broustis et al., 2007; Broustis et al., 2011; Rosier et al., 2010; Lu et al., 2005b; Zhejiang et al., 2008). MAC protocols for UWB are classified into two main categories: centralised and distributed MAC protocols. Centralised MAC protocols uses a central controller like a base station or access point to control data transmission between devices. However, in distributed MAC protocol, data packets are transmitted between nodes independently with no central guidance to avoid central point of failure and central synchronisation (Zin and Hope, 2010; Hu et al., 2010; Gupta and Mohapatra, 2007).

Mathematical analysis is one of most important tools employed to evaluate the performance of MAC protocols designed for UWB networks. Performance evaluation of MAC protocols of UWB technology addresses many measures including bit error rate, delay analysis, packet loss probability, queue length, and throughput. Packet loss probability increases when the number of collisions increases. Thus, attaching buffers at nodes is an important reason to reduce packets loss (Broustis et al., 2007; Liu et al., 2009; Rajamani et al., 2008; Han, 2013; Liu et al., 2008; Chen et al., 2006; Aripin et al., 2009). In Liu et al. (2009) authors proposed a discrete-time single server queue with vacation model for the distributed reservation protocol defined in the WiMedia MAC to allow channel time being reserved in a distributed manner under different reservation patterns. Authors took into account the dynamics of UWB shadowing channel. However, the queueing model is developed for a single band UWB MAC protocol only. In Broustis et al. (2007), a theoretical analysis for a distributed multi-band MAC protocol of UWB clique topology is introduced. The authors provided insight with regard to whether bands are all efficiently utilised or not. The effects of buffer and, in particular, delay and loss probability were not taken into consideration. The evaluation process was developed in terms of stability and the uniform usage of the different bands.

In Rajamani et al. (2008), authors investigated ECMA-368 MAC performance for extended data rates. They shown that, throughput is improved at these extended PHY rates. This improvement is a function of the transfer size. They also shown that scaling PHY frame size does not improve throughput for bad channels. In Han (2013), authors proposed a queueing model to analyse the performance of WiMedia system with frame aggregation of video traffic. In Chen et al. (2006), the authors studied the delay performance of the Dly-ACK scheme. An analytical model was developed for the Dly-ACK mechanism, and the delay was decomposed into queuing and delivery delay. These delay metrics were derived, and some important observations were obtained. In particular, they considered an optimal burst size, which was determined by the input traffic load and is very insensitive to the channel error rate within a normal error-rate range. They, also, demonstrated that Dly-ACK cannot work properly if the burst size is fixed. The authors then proposed a dynamical Dly-ACK scheme that can adaptively change its burst size according to the queue buffer size. Simulation results shown that the dynamical scheme can improve the delay performance significantly. In Aripin et al. (2009), the authors proposed cross layer framework of video transmission over cognitive radio UWB. Then, a simulation study is carried out to evaluate the effect of resource allocation at the MAC layer to the video quality perceived at the receiver.

Park et al. (2016) suggested an analytical model for the sending activities of machine to machine devices with directional UWB antennas. Moreover, they considered both the deafness problem of directional area and the steady-state probability of the different states of directional-CSMA-CA scheme. Also, they introduced the differentiated service of channel access algorithm by joining different frame payload size of back-off period. In addition, they demonstrated that the proposed dynamic adaptation of directional-CSMA-CA scheme enhances the saturated throughput compared with the legacy directional-CSMACA mechanism. However, the authors did not utilise the characteristics of UWB signals. In our work, we will employ widely the unique features of UWB signals.

Ouanteur et al. (2017a) suggested a discrete time Markov chain model to represent a single node using the low latency deterministic networks (LLDNs) mode to transmit its data packet. They provided a comprehensive analysis of the LLDN profile specified in IEEE 802.15.4e considering the dedicated timeslots in retransmission. However, the authors did not consider number of bands. In the current paper, we will use multiple bands to optimise usage of the available BW.

Ouanteur et al. (2017b) presented an enhancement analytical study of the transmission in the shared link using time slotted channel hopping with collision avoidance (TSCH CA) algorithm. They considered the deterministic behaviour of the TSCH mechanism. Then, they studied the effect of the number of devices sharing the same channel on

the efficiency of the network, under non-saturated situations. However, the authors assumed ideal channel, single band MAC, and star topology. In the current paper, we alleviate this restriction via assuming clique topology which utilise multi-band MAC protocol with non-ideal channel.

Mohammed et al. (2017) solved the problem of multi-user interference (MUI) appears in the IR-UWB communication applied to WPANs. They solved the mentioned problem via suggesting a new correlation technique. However, they assumed a centralised MAC protocol and used only a symbol error rate as a performance metric. In our work, we will consider distributed multi-band MAC protocol and assume many performance metrics.

The contributions of our paper are three folds: first, we introduce a new queueing model framework to evaluate the performance of the distributed multi-band MAC protocol for a multi-band UWB WPAN. Second, we derive an expression for the probability that a certain node wins a contention on a valid receiver and a free band. Third, we introduce strategies to remove random choice of both receivers and bands. The remainder of this paper is organised as follows: Section 2 gives an overview of the considered MAC protocol. Section 3 introduces the model assumptions. An extensive mathematical analysis of the proposed model is introduced in Section 4 where a set of difference equations needed to obtain the performance metrics. An expression for the probability of wining contention is derived in Section 5. The performance metrics are derived in Section 6. The numerical results and simulation are conducted in Section 7. The conclusion is introduced in Section 8.

2 Overviews of multi-band MAC protocol

As aforementioned, this paper introduces a queueing model framework aiming to find suitable formula to reflect the system behaviour of an existing multi-band MAC protocol in UWB networks, particularly, a protocol which is used to increase both band utilisation and throughput. In Broustis et al. (2007), the authors proposed a MAC protocol for use in multi-hop wireless networks that deploy an underlying UWB-based physical layer. They considered a multi-band approach to better utilise the available spectrum, where each transmitter sends longer pulses in one of many narrower frequency bands. We will capture most of the assumptions introduced in Broustis et al. (2007) and we just refer to those effect mainly on our work. In Broustis et al. (2007), the available BW is divided into B bands, one of which named *REQ-band* is used to manage the control requests and negotiation about the data transmissions. The *REQ-band* is used during what is called *REQUES* state. The remaining $B-1$ bands are used in data transmissions during what is called *TALK* state. The requests of transmissions are managed by control packets referred to as *REQ* packets. The *REQ* packets are sent during the time hopping sequences (THSs) of receivers. Moreover, the channel time axis is divided into superframes separated by availability frames.

Figure 1 Frame structure

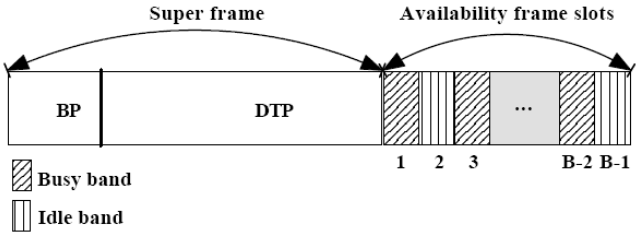

As shown in Figure 1, the superframes consists of a beacon period (BP) which containing timing and control information, and a data transfer period (DTP). The availability frames are used to declare the occupied bands and free bands during what is called *DECLARE* state. Upon having system information, nodes transmit their data packets to their target corresponding receivers using randomly selected bands. Collisions may occur if one of the following two cases occurs:

1 *at receiver:* collision happens when a receiver is selected by more than one sender

2 *at bands:* collision happens when a band is selected by more than one sender at the same time for transmission.

When collisions occur, the colliding senders transfer into a *BACK-OFF* state and wait some time before sending a new transmission request. This waiting time is named *BACK-OFF* time. The *BACK-OFF* time is determined by a suitable *BACK-OFF* algorithm. Actually, we use exponential *BACK-OFF* algorithm in this paper. Senders that are in the *BACK-OFF* state cannot transmit data but they are allowed to receive data.

Figure 2 The transition diagram of the protocol operations

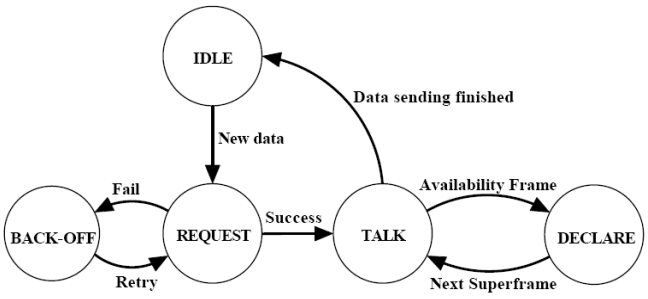

Figure 2 illustrates a node transition diagram of the protocol operations (Broustis et al., 2007). Although, the UWB technology can be used in multi-hop ad hoc networks, we assume in this analysis that all nodes are within the same transmission range. That is, we consider a *clique* topology. The analysis becomes much more complex and intractable in a multi-hop setting (Broustis et al., 2007).

3 Model assumptions

The proposed model is analysed based on the following assumptions:

1 The time axis is divided into slots, each equal to the time of negotiation process and the time of transmission one packet. Non negative integers $k = 0, 1, \ldots$ are assigned to the individual slot boundaries. Time interval $(k, k + 1)$ is referred to as slot $k + 1$. Each time slot consists of two parts. The first part denotes the availability frame which reflects the bands' status. The second part represents the superframe which is long enough to transmit a data packet. A small time of the superframe is used in rendezvous process while most of the superframe time is used in data transmission. The availability frame is too short compared to the superframe frame.

2 Each node has a buffer of finite capacity C to host the arriving packets. The packets are moved one by one until arriving head of queue.

3 Packets arrive into nodes as a Bernoulli process. That is at the beginning of every slot k a packet will arrive with probability β and will not arrive with probability $\overline{\beta} = 1 - \beta$. This implies that packets arrival rate at a node is β per slot, and that the packet inter-arrival time is geometrically distributed with expectation $\frac{1}{\beta}$ slots.

4 Let L be the maximum number of collisions (i.e., the maximum number of retransmission trails for each node due to collisions) after which a packet is dropped automatically.

5 The state of the system is captured at the end of each superframe just after the availability frame.

6 If a sender has a packet to send, at the start of a slot k, it selects one of the available bands randomly and send a REQ packet to the required receiver via the REQ band.

7 Packets are arranged together to form messages.

8 The service time is defined as the time required to transmit a message from sender to receiver.

9 Packets are arranged together to form messages.

10 Let $X^k = 1, 2, \cdots$ be a RV denoting the *service time* of a message at slot k. The *service time* is defined as the time required to transmit a message from sender to receiver. We assume that the RV X^k is geometrically distributed with $x_i^k = \Pr[X^k = i]$ given as $x_i^k = s^{-i-1}s$, where $\overline{s} = 1 - s$.

4 Model analysis

For simplicity, we assume that all the nodes in the *clique* topology are statistically identical and independent. For a certain node under consideration (called *tagged sender*) and an arbitrary slot k, let $P_1^k = 0, 1, 2, \cdots, C$ be a RV represents the number of buffered packets at the *tagged sender*. Let $P_2^k = 0, 1$ be a RV denotes the transmission state of the *tagged sender* in slot k. The RV $P_2^k = 0$ means that the *tagged sender* in *IDLE*, *REQUEST* or *BACK-OFF* state, while $P_2^k = 1$ means a message is being served at the *tagged sender*. Let P_3^k be a RV representing the backoff stage [0, 1, ⋯, L], i.e., the number of collisions, for the *tagged sender* at slot k; where L is the maximum number of message retry limit. When a collision occur at the *tagged sender*, it generates a backoff time, which is a uniform RV between 1 and W, where $W = 2^L$ is the window size. Let $P_4^k = 1, 2, \cdots, W$ be a RV represents the backoff timer for the *tagged sender*. Unlike the mathematical model introduced in Broustis et al. (2007), we introduce a 4-D Markov model where each node is modelled by a 4-tuple $(P_1^k, P_2^k, P_3^k, P_4^k)$. The process $\{(P_1^k, P_2^k, P_3^k, P_4^k),\ k = 0, 1, 2, \ldots\}$ forms a 4-D, discrete-time Markov model (Nassar, 1995; Nassar and Al-Mahdi, 2009, 2003; Nassar and Fouad, 2003) with state space given as:

$$S = \{(i, j, l, m) | 0 \le i \le C, 0 \le j \le 1, 0 \le l \le L, 1 \le m \le 2^L\} \quad (1)$$

This enables us to characterise the quality of service (QoS) of performance metrics, such as queue length, blocking probability, dropping probability, collision probability, wining contention probability and delay for the UWB MAC protocol systems with finite buffer capacity. Let $p_{i,j,l,m}^k = \Pr[P_1^k = i, P_2^k = j, P_3^k = l, P_4^k = m]$ be the transient distribution of that chain at slot k. This transient distribution can be evaluated by knowing the state of the *tagged sender* at the end of slot $k - 1$. The state transition diagrams of this 4-D Markov chain model is depicted in Figure 3.

The parameter m, which represents the backoff timer, is decremented by 1 after each slot elapsed until reaches to zero. In each slot k, just after massage arrival instant, the *tagged sender* wins the contention to transmit its message with probability α^k and does not win the contention with probability $\overline{\alpha}^k = 1 - \alpha^k$. The value of α^k will be derived in Section 5. The transition diagrams in Figure 3 have circles, which represent the states the *tagged sender* can be in, and directed arcs which represent the transitions between these states. The probability that this transition is made as time advances from one slot to the next is written next to each transition. To illustrate this, consider state (1, 1, 0, 0) in Figure 3, which means that the *tagged sender* has one packet in its queue, out of which one packets is being served, the number of collisions is 0 and the backoff time is 0. This state will be reached in a certain slot $k + 1$ if the *tagged sender* in the previous slot k is in any one of the following states and some event occurs.

1 States $(1, 0, l, 0)$, $0 \le l \le L$. Starting from those states, state (1, 1, 0, 0, 0) takes place if no packet arrived with probability $\overline{\beta}$ at the start of slot $k + 1$ AND the *tagged sender* wins the contention to transmit its packets during slot $k + 1$ with probability α^{k+1}.

2 States (1, 1, 0, 0). Starting from those states, state (1, 1, 0, 0, 0) takes place if no packet is arrived with probability $\overline{\beta}$ at the start of slot $k + 1$ AND no packet served at the end of slot $k + 1$.

Figure 3 The transition diagram (see online version for colours)

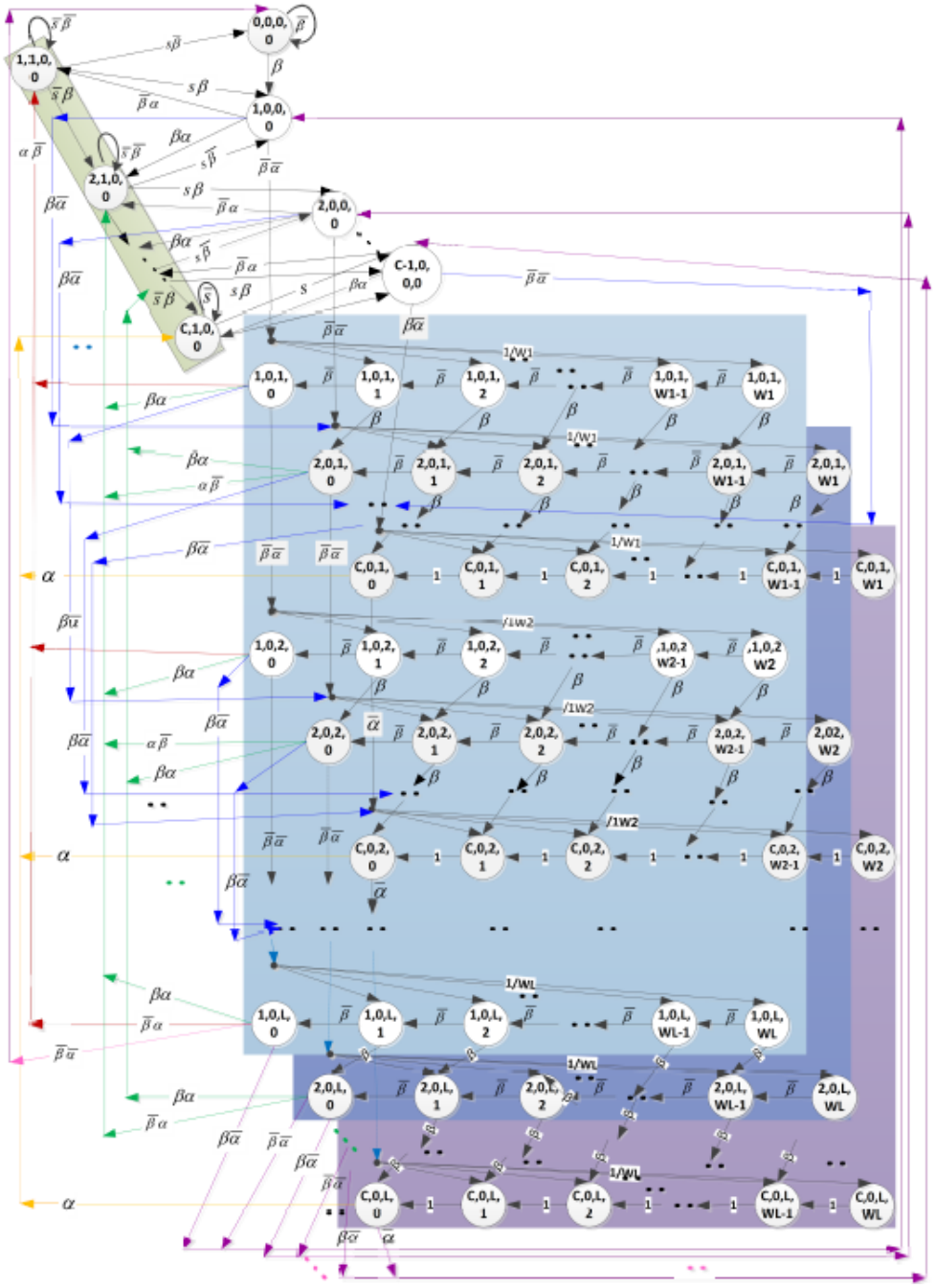

The transition diagram shows how the difference equations listed below are derived. In what follows, we derive a set of equations that collectively form a difference equation defining the distribution $P^k_{i,j,l,w}$. From the transition diagram in Figure 3, one can write:

$$p^{k+1}_{0,0,0,0} = p^k_{0,0,0,0}\overline{\beta} + p^k_{1,1,0,0}\overline{\beta}s \tag{2}$$

$$+p^k_{1,0,L,0}\overline{\beta}\overline{\alpha}^k \tag{3}$$

The transient states $p^{k+1}_{i,0,0,0}, 1 \le i \le C$ can be given as follows:

$$p^{k+1}_{i,0,0,0} = \begin{cases} p^k_{i-1,0,0,0}\beta + p^k_{i,1,0,0}s\beta + p^k_{i+1,1,0,0}s\overline{\beta} + p^k_{i,0,L,0}\beta\overline{\alpha} + p^k_{i+1,0,L,0}\overline{\alpha}\overline{\beta} & i=1 \\ p^k_{i,1,0,0}s\beta + p^k_{i+1,1,0,0}s\overline{\beta} + p^k_{i,0,L,0}\overline{\alpha}\beta + p^k_{i+1,0,L,0}\overline{\alpha}\overline{\beta} & 2 \le i < C-1 \\ p^k_{i,1,0,0}s\beta + p^k_{i+1,1,0,0}s\overline{\alpha} + p^k_{i,0,L,0}\overline{\alpha}\beta + p^k_{i+1,0,L,0}\overline{\beta} & i = C-1 \end{cases} \tag{4}$$

For $i = 1$ and $1 \le l \le L$, we have:

$$p^{k+1}_{1,0,l,0} = p^k_{1,0,l,1}\overline{\beta} \tag{5}$$

For $1 < i < C$ and $1 \le l \le L$ we have:

$$p^{k+1}_{i,0,l,0} = p^k_{i,0,l,1}\overline{\beta} + p^k_{i-1,0,l,1}\beta \tag{6}$$

For $i = C$ and $1 \le l \le L$ we have:

$$p_{C,0,l,0}^{k+1} = p_{C,0,l,1}^{k} + p_{C-1,0,l,1}^{k}\beta \tag{7}$$

For $1 \le l \le L$ and $1 \le w < W_l$, we have:

$$p_{1,0,l,w}^{k+1} = p_{1,0,l,w+1}^{k}\overline{\beta} + \frac{1}{W_l} p_{1,0,l-1,0}^{k}\overline{\beta}\overline{\alpha} \tag{8}$$

For $1 \le l \le L$, we have:

$$p_{1,0,l,W_l}^{k+1} = \frac{1}{W_l} p_{1,0,l-1,0}^{k}\overline{\beta}\overline{\alpha} \tag{9}$$

For $1 < i < C$, $1 \le l \le L$ and $1 \le w \le W_l$ we have:

$$\begin{aligned} p_{i,0,l,w}^{k+1} &= \left(p_{i,0,l,w+1}^{k}\overline{\beta} + p_{i-1,0,l,w+1}^{k}\beta \right) \\ &\quad + \frac{1}{W_l}\left(p_{i,0,l-1,0}^{k}\overline{\beta}\overline{\alpha} + p_{i-1,0,l-1,0}^{k}\beta\overline{\alpha} \right) \end{aligned} \tag{10}$$

For $1 < i < C$ and $1 \le l \le L$, we have:

$$p_{i,0,l,W_l}^{k+1} = \frac{1}{W_l}\left(p_{i,0,l-1,0}^{k}\overline{\beta}\overline{\alpha} + p_{i-1,0,l-1,0}^{k}\beta\overline{\alpha} \right) \tag{11}$$

For $1 \le w < W_l$, we have:

$$p_{C,0,1,W_l}^{k+1} = \left(p_{C,0,l,w+1}^{k} + p_{C-1,0,l,w+1}^{k}\beta \right) + \frac{1}{W_l} p_{C-1,0,0,0}^{k}\beta\overline{\alpha} \tag{12}$$

For $2 \le l \le L$ and $1 \le w < W_l$, we have:

$$\begin{aligned} p_{C,0,l,w}^{k+1} &= \left(p_{C,0,1,w+1}^{k} + p_{C-1,0,1,w+1}^{k}\beta \right) \\ &\quad + \frac{1}{w_l} p_{C-1,0,l-1,0}^{k}\beta\overline{\alpha} + \frac{1}{w_l} p_{C,0,l-1,0}^{k}\overline{\alpha} \end{aligned} \tag{13}$$

For $L = 1$ and $i = C$, we have:

$$p_{C,0,1,W_1}^{k+1} = \frac{1}{w_1} p_{C-1,0,0,0}^{k}\beta\overline{\alpha} \tag{14}$$

For $2 \le l \le L$, we have:

$$p_{C,0,l,W_l}^{k+1} = \frac{1}{W_l}\left(p_{C,0,l-1,0}^{k}\overline{\alpha} + p_{C-1,0,l-1,0}^{k}\beta\overline{\alpha} \right) \tag{15}$$

The probabilities $p_{i,1,0,0}^{k+1}$ for $1 \le i \le C$ can be given as follows.

$$p_{i,1,0,0}^{k+1} = \begin{cases} p_{i,1,0,0}^{k}\overline{\beta}\overline{s} + \sum_{l=0}^{L} p_{i,0,l,0}^{k}\overline{\beta}\alpha^{k} & i = 1 \\ p_{i,1,0,0}^{k}\overline{\beta}\overline{s} + p_{i-1,1,0,0}^{k}\overline{s}\beta \\ \quad + \sum_{l=0}^{L} p_{i-1,0,l,0}^{k}\beta\alpha^{k} + p_{i,0,l,0}^{k}\overline{\beta}\alpha^{k} & 2 \le i < C \\ p_{i,1,0,0}^{k}\overline{s} + p_{i,0,0,0}^{k}\alpha^{k+1} + p_{i-1,1,0,0}^{k}\overline{s}\beta \\ \quad + \sum_{l=1}^{L}\left(p_{i,0,l,0}^{k}\alpha^{k} + \beta p_{i-1,0,l,0}^{k}\alpha^{k} \right) & i = c \end{cases} \tag{16}$$

Note that:

- $p_{0,0,l,w}^{k+1} = 0$ for $l + w > 0$, since it is meaningless to count for an empty system.
- $p_{i,0,0,w}^{k+1} = 0$ for $w > 0$, since it is meaningless to count without contentions or collisions.
- $p_{i,1,l,w}^{k+1} = 0$ for $l + w > 0$, since it is meaningless to count as a backoff state while a packet is actually in the service.
- $p_{0,1,l,w}^{k+1} = 0$ for $l + w \ge$ `0, since it is meaningless to have a packet in the server while actually no packets in the system at all.
- $p_{C,0,0,0}^{k+1} = 0$ since it is impossible to reach state (C, 0, 0, 0) from any of the other states. For example, if the system in state ($C - 1$, 0, 0, 0)at the end of slot k (i.e., at the start of slot $k + 1$) then either one of the following events will occur:

1 A new packet arrives at the start of slot $k + 1$ with probability β. In such case, a sender will compete for transmission just after the arrival instance. The sender either wins contention by the end of slot $k + 1$ and becomes in state (C, 1, 0, 0) or the sender loss the contention, it will be in state (C, 0, 1, w), $w = 1, 2$.

2 A new packet does not arrive with probability $\overline{\beta}$. In such case, a sender will compete for a transmission at the start of slot $k + 1$. The sender either wins contention and sends the packet and becomes in state ($C - 1$, 1, 0) or the sender loss the contention, the state will be ($C - 1$, 0, 1, w), $w = 1, 2$.

Algorithm 1 Parameters initialisation

1: $\varepsilon \leftarrow 10^{-9}$ and $k \leftarrow 0$	{Initialise the convergence threshold and the start of loop}.
2: **for all** i, j, w, l **do**	
3: **if** $i + j + l + w = 0$ **then**	
4: $p_{i,j,w,l}^{k} \leftarrow 1$	{Initilise $p_{0,0,0,0}^{0}$ to 1}.
5: **else**	
6: $p_{i,j,w,l}^{k} \leftarrow 0$	{Initilise $p_{i,j,w,l}^{0}$ to 0}.
7: **end if**	
8: **end for**	
9: $\psi_0^0 \leftarrow 1, \psi_j^0 \leftarrow 0, 1 \le j \le B - 1$.	
10: Input the values of β, s, L, C, M.	{Initilise the operational parameters}.

Algorithm 2 Steady-state calculations

1: **repeat**
2: *Compute* λ_1^k, λ_2^k using (31) and (32). {Calculate the arrival rates at loop k}
3: Pr $[H^K = n \mid \Psi^{k-1} = m, S^k = l]$ using (26).
4: Compute $d_{j|m,v}^{k+1}$ using (28).
5: Compute Pr $[S^{k+1} = l \mid \Psi^k = m]$; $m = 0, 1, 2, \ldots, B-1$; $l = 0, 1, 2, \ldots, M-2m$ using (33).
6: Compute ψ_j^{k+1}, $j = 0, 2, \ldots, B-1$ from (29) and (30).
7: Compute α^k using (23).
8: Compute the new values of $p_{i,j,l,w}^{k+1} \forall_{i,j,l,w}$.
9: $flag \leftarrow 0$
10: **for all** i, j, k, l such that $i + j + k + l <= B$ **do**
11: **if** $\left| p_{i,j,w,l}^{k+1} - p_{i,j,w,l}^{k} \right| > \kappa$ **then**
12: $flag \leftarrow 1$ {If the steady-state is not reached, set $flag = 1$}
13: **end if**
14: **end for**
15: **for all** i, j, w, l **do**
16: $p_{i,j,w,l}^{k} \leftarrow p_{i,j,w,l}^{k+1}$ {Update the value of the probabilities $p_{i,j,w,l}^{k}$ }
17: **end for**
18: **until** $flag = 0$
19: The steady state probabilities are obtained.

To fully solve the previous system of difference equations, we will embark on finding an expression value for α^k in the next section. First, we iteratively compute the steady-state system occupancy $p_{i,j,l,w}$ using Algorithm 1 and 2. The initialisation parameters are executed using Algorithm 1, while the steady-state probabilities are calculated using Algorithm 2. This algorithm stopped when the steady-state probabilities $p_{i,j,w,l}^{k}$ are reached. Upon the steady state system occupancy is reached, it is easily to compute the aforementioned performance metrics.

5 Deriving the contention wining probability

The main objective of this section is to find a formula for the probability α^k that the *tagged sender* wins the contention on a valid receiver and a free band at start of slot k. As a result, it can establish a connection with an available receiver and starts its transmission during slot k. We consider M nodes, including the *tagged sender*, where each node is equipped with one transmitter and one receiver. Let $S^k = 0, 1, 2, \ldots, M$ be a RV denoting the number of senders in *REQUES* state at start of slot k (i.e., having packets to be sent) including the *tagged sender*. Let $\Psi^k = 0, 1, 2, \ldots, B-1$ be a RV denoting the number of busy bands at the start of slot k. If Ψ^k is the number of occupied bands, then there are $2 \times \Psi^k$ nodes actively engaged in some session as a sender or a receiver (Broustis et al., 2007). The number of valid receivers is given as $r_{l,m}^k = M - l - 2m$, where $l = 0, 1, 2, \ldots, S^k$ and $m = 0, 1, 2, \ldots, \Psi^k$. The valid receiver must be in the *IDLE* or *BACKOFF* state. Let $R_{success}^k = 0, 1, 2, ..., r_{l,m}$ be a RV denoting the number of picked valid receivers such that each one is requested by exactly one sender in the *REQUES* sate at slot k. If $\Psi^k < B - 1$ and $S^k \geq 1$, then the *tagged sender* will success to establish a new session if the following two conditions occur:

1 *condition 1:* it selects one of the valid receivers as a target receiver and non of the remaining other $S^k - 1$ senders, in the *REQUEST* state, select the same valid receiver as a target (otherwise, more than one sender will use the same THS to send their requests, causing a collision)

2 *condition 2:* non of the $S^k - 1$ senders, that have been successfully delivered their *REQ* control messages to a different target receivers, selects the same free data band which selected by the *tagged sender*.

Toward this, the derivation of the probability α^k will be done in three stages. In first stage, we will derive the probability distribution of the number of senders which select a valid receiver as a target receiver. In other words, there is no valid receiver was chosen by more than one sender as a target. In second stage, out of the number of senders success in first stage, we will derive the probability distribution of the number of senders success to select a free data band such that no free data band is selected by more than one sender for data transmission. In the third stage, based on the first and second stages, we will derive the probability α^k that the *tagged sender* establishes a new session. Below, we will embark on deriving the probabilities in the previous three stages in details.

5.1 First stage

In this stage, the probability $\Pr[R_{success}^k = i \mid \Psi^k = m, S^k = l]$ will be derived, where $l = 0, 1, \ldots, M-2m$ and $m = 0, 1, \ldots, B-1$. Let $e_w^k, w = 1, 2, ..., r_{l,m}^k$ be integers variables denoting the number of senders that select the same receiver w as a valid receiver, where $0 \leq e_w \leq S^k$ and:

$$e_1^k + e_2^k + \cdots + e_{r_{l,m}^k}^k = S^k \tag{17}$$

The number of w-set combinations of the set $G^k = \left(e_1^k, e_2^k, \cdots, e_{r_{l,m}^k}^k\right)$ which represents the number of non-negative integer solutions of equation (17) is given as $C(S^k + r_{l,m}^k - 1, r_{l,m}^k - 1)$ (Rosen, 1999), where $C(x, y) = \dfrac{x!}{y!(x-y)!}$ is the number of permutations of x things taken y at a time. In other words, the value $C(S^k + r_{l,m}^k - 1, r_{l,m}^k - 1)$ represents the number of sequences that G^k can be formed. As aforementioned, the valid

receiver may be not selected by senders (i.e., $e_w^k = 0$), selected by exactly one sender (i.e., $e_w^k = 1$) OR selected by more than one sender (i.e., $e_w^k \geq 2$). Note that, not all the S^k senders select valid receivers. In other words, some senders may select valid receivers while others do not. Let $H^K = 0, 1, \cdots, S^k$ be a RV denoting the number of senders which select valid receivers while the remaining $S^k - H^k$ senders select invalid receivers. Thus, without loss of generality, we have the following three subsets groups out of G^k:

1 The subset A of size i represent number of receivers which are selected by exactly one sender (i.e., $e_w^k = 1$). The number of permutations of $r_{l,m}^k$ taken i at a time is $C(r_{l,m}^k, i)$, where $i = 0, 1, 2, ..., \min(r_{l,m}^k, n)$, $n = 0, 1, \ldots, l$, $l = 0, 1, \ldots, M$ and $\sum_{w=1}^{i} e_w^k = i$.

2 The subset B of size j represents number of receivers which are not selected by any sender (i.e., $e_w^k = 0$). The number of permutations of $r_{l,m}^k - i$ taken j at a time is $C(r_{l,m}^k - i, j)$, $j = 0, 1, ..., r_{l,m}^k - i$.

3 The subset C represents number of receivers which are selected by more than one sender (i.e., $e_w^k \geq 2$). The number of sequences, that the subset C can be formed, is given as follows. Substituting for elements of the subsets A, B and C into (17) and letting $S^k = n$ then we get:

$$\underbrace{1+1+\ldots+1}_{i}+\underbrace{0+0+\ldots+0}_{j} + \underbrace{e_{i+j+1}+e_{i+j+2}+\ldots+e_{\eta,m}}_{\eta,m-i-j} = n \tag{18}$$

which gives:

$$\underbrace{e_{i+j+1}^k+e_{i+j+2}^k+\ldots+e_{\eta,m}^k}_{r_{l,m}^k-i-j} = n-i \tag{19}$$

Therefore, without loss of generality, we can rewrite (19) as:

$$e_1^k+e_2^k+\ldots+e_{r_{l,m}^k-i-j}^k = n-i \tag{20}$$

The number of integer solutions of (20) where $e_r \geq 2$, $r = 1, 2, \ldots, r_{l,m} - i - j$ is given from [28] as:

$$C\left(r_{l,m}^k - i - j + n - i - 1 - 2 - 2 - \ldots - 2, r_{l,m}^k - i - j - 1\right) = C\left(n - r_{l,m}^k + j - 1, r_{l,m}^k - i - j - 1\right)$$

The probability distribution $\tau_{i|m,l,n}^k = \Pr[R_{success}^k = i \mid \Psi^k = m, S^k = l, H^k = n]$ can be given as:

$$\tau_{i|m,l,n}^k = \begin{cases} 1 & if\ r_{l,m}^k = 0, i = 0 \\ 0 & if\ r_{l,m}^k = 0, i > 0 \\ \dfrac{C\left(r_{l,m}^k, i\right)}{\left(r_{l,m}^k\right)^n} \sum_{j=0}^{r_{l,m}^k - i} C\left(r_{l,m}^k - i, j\right) & if\ r_{l,m}^k > 0 \\ C\left(n - r_{l,m}^k + j - 1, r_{l,m}^k - i - j - 1\right) & \\ \times \sum_{\delta=1} \dfrac{n!}{\prod_{w=1}^{r_{l,m}^k - i - j} e_w^k!} & \end{cases} \tag{21}$$

where $i = 0, 1, ..., \min(r_{l,m}^k, n)$, $n = 0, 1, \ldots, l$, $l = 0, 1, \ldots, M - 2m$, $C\left(r_{l,m}^k, i\right)$ is the number of valid receivers such that $e_i^k = 1$, $C(r_{l,m}^k - i, j)$ is the number of valid receivers such that $e_i^k = 0$ and $C(n - r_{l,m}^k + j - 1, r_{l,m}^k - i - j - 1)$ is the number of valid receivers be formed satisfying $\sum_{w=1}^{r_{l,m}^k - i - j} e_w^k = n - i$.

5.2 Second stage

Similar to the first stage, we derive an expression for probability distribution of the number of senders that uniquely success to obtain a free band, i.e., there is no free data band is chosen by more than one sender. In this case, the number of available free bands is given as $b_m^k = B - m - 1$, $m = 0, 1, \ldots, \Psi^k$. Let $\Omega_{success}^k = 0, 1, \cdots b_m^k$ be a RV denoting the number of picked bands such that each band is requested by exactly one sender in the *REQUES* state at slot k. The number of senders in this case is reduced to the number of senders that was successfully delivered their *REQ* packets to their targets in the first stage. Hence, the probability distribution $\omega_{v|m,l,i,n}^k = \Pr[\Omega_{success}^k = v \mid \Psi^{k-1} = m, S^k = l, R_{success}^k = i, H^k = n]$ is given for $0 \leq v \leq \min(B - m - 1, i)$ as:

$$\omega_{v|i,m,l,n}^k = \begin{cases} 1 & \text{if } b_m^k = 0, v = 0 \\ 0 & if\ b_m^k = 0, v > 0 \\ \dfrac{C\left(b_m^k, v\right) i!}{\left(b_m^k\right)^i} \sum_{f=0}^{b_m^k - v} C\left(b_m^k - v, f\right) & if\ b_m^k > 0, v \geq 0 \\ \times \sum_{\zeta=1}^{C(i - b_m^k + f - 1, b_m^k - v - f - 1)} \dfrac{1}{\prod_{w=1}^{b_m^k - v - f} \hat{e}_w^k!} & \end{cases} \tag{22}$$

where $\hat{e}_w^k$ are integers variables denoting the number of senders that select the same band w and $\hat{e}_1^k + \hat{e}_2^k + \cdots + \hat{e}_{b_m^k}^k = i - v$ with the number of integer solutions given as $C(i - b_m^k + f - 1, b_m^k - v - f - 1)$.

5.3 Third stage

In equation (22), we derived the probability distribution of the number of senders that are succeeded in establishing successful sessions. Actually, sometimes we have a number of successful sessions while the tagged sender is not included between those successful senders. Therefore, we must obtain the probability that the tagged sender is between those successful senders; that is the probability that the tagged sender succeeded to establish a successful session. The probability α^k that a tagged sender succeeded to establish a successful session is given as:

$$\begin{aligned}\alpha^k = & \sum_{m=0}^{\min\left(B-1,\left\lfloor\frac{M}{2}\right\rfloor\right)} \sum_{l=1}^{M-2m} \sum_{n=1}^{l} \sum_{i=1}^{\min(\eta_{,m},n)} \sum_{v=1}^{\min(\eta_{,m},n,B-1-m)} \\ & \Pr\begin{bmatrix} Success(1,2) \mid \Omega_{success}^k = v, \\ \Psi^{k-1} = m,\ S^k = l, \\ R\_Success = i,\ H = n \end{bmatrix} \\ & \times \omega_{v|i,m,l,n}^k \tau_{i|m,l,n}^k \Pr\left[H^K = n \middle| \Psi^{k-1} = m,\ S^k = l\right] \\ & \times \Pr\left[S^k = l \middle| \Psi^{k-1} = m\right] \times \Pr\left[\Psi^{k-1} = m\right]\end{aligned} \tag{23}$$

where *Success*(1, 2) means the tagged node successes in stages 1 and 2. It is easy to deduce that:

$$\Pr\left[Success(1,2) \middle| \Omega_{success}^k = v,\ \Psi^{k-1} = m,\ S^k = l\right] = \frac{v}{l} \tag{24}$$

The conditional probability distribution $\Pr[H^K = n \mid \Psi^{k-1} = m, S^k = l]$ is given as:

$$\Pr\left[H^K = n \middle| \Psi^{k-1} = m,\ S^k = l\right] \tag{25}$$

$$= C(l,n)\left(\frac{r_{l,m}^k}{M-2m}\right)^n \left(1-\frac{r_{l,m}^k}{M-2m}\right)^{l-n},\ n = 0, 1, 2, \cdots, l \tag{26}$$

It is remains for us to derive an expression for the probability distribution $\Pr[\Psi^k = m]$ and $\Pr[S^k = l \mid \Psi^{k-1} = m]$. Toward this, let D^k be a RV denoting the number of bands switched from busy to idle state at the end of slot k (i.e., the number of senders finish their transmission at the end of slot k). The state of each band can be modelled as Bernoulli trial where at the end of slot k, a busy band is released with probability s or not with probability $1 - s$. It clears that, the value of the RV D^k depends on the values of the RVs Ψ^{k-1} and $\Omega_{success}^k$. Then the $d_{j|m,v}^k$ of the RV D^k is given as:

$$d_{j|m}^k = \Pr\left[D^k = j \middle| \Psi^{k-1} = m\right] \tag{27}$$

The RV D^k follows the binomial distribution with parameters m, j and s which can be written as:

$$d_{j|m}^k = C(m, j) s^j s^{-m-j},\ m = 0, 1, 2, ..., \min\left(B-1, \left\lfloor\frac{M}{2}\right\rfloor\right) \tag{28}$$

The distribution of $\psi_j^k, j = 0, 1, 2, ..., \min\left(B-1, \left\lfloor\frac{M}{2}\right\rfloor\right)$, is given as follows. For $j = 0$, we have:

$$\begin{aligned}\psi_0^k = \Pr[\Psi^k = 0] = & \sum_{m=0}^{\min\left(B-1,\frac{M}{2}\right)} \sum_{l=0}^{M-2m} \sum_{n=0}^{l} \sum_{i=0}^{\min(\eta,m,n)} \omega_{0|i,m,l,n}^k \\ & \times d_{m|i,m,l,n}^k \times \tau_{i|m,l,n}^k \Pr\left[H^K = n \middle| \Psi^{k-1} = m,\ S^k = l\right] \\ & \times \Pr\left[S^k = l \middle| \Psi^{k-1} = m\right] \times \Pr\left[\Psi^{k-1} = m\right]\end{aligned} \tag{29}$$

For $j = 1, 2, ..., \min\left(B-1, \left\lfloor\frac{M}{2}\right\rfloor\right)$, we have:

$$\begin{aligned}\psi_j^k = \Pr[\Psi^k = j] = & \sum_{m=0}^{j-1} \sum_{l=j}^{M-2m} \sum_{n=0}^{l} \sum_{i=0}^{\min(\eta,m,n)} \sum_{h=0}^{m} \omega_{j-m+h|i,m,l,n}^k \\ & \times d_{h|i,m,l,n}^k \times \tau_{i|m,l,n}^k \Pr\left[H^K = n \middle| \Psi^{k-1} = m,\ S^k = l\right] \\ & \times \Pr\left[S^k = l \middle| \Psi^{k-1} = m\right] \times \Pr\left[\Psi^{k-1} = m\right] \\ & + \sum_{m=j}^{\min\left(B-1,\left\lfloor\frac{M}{2}\right\rfloor\right)} \sum_{l=j}^{M-2m} \sum_{n=0}^{l} \sum_{i=0}^{\min(\eta,m,n)} \sum_{h=0}^{m} \omega_{h|i,m,l,n}^k \\ & \times d_{m-j+h|i,m,l,n}^k \times \tau_{i|m,l,n}^k \Pr\left[H^K = n \middle| \Psi^{k-1} = m,\ S^k = l\right] \\ & \times \Pr\left[S^k = l \middle| \Psi^{k-1} = m\right] \times \Pr\left[\Psi^{k-1} = m\right]\end{aligned} \tag{30}$$

Now, we embark on finding he value of the probability $\Pr[S^k = l \mid \Psi^{k-1} = m]$ as follows. We have to note that, the existing nodes can be grouped into two classes. The first class of size i, $i = 0, 1, \ldots, M - 2m$, contains the nodes that did not in the *BACK-OFF* state and have packets to be send at the start of slot k plus empty buffer nodes with new arrivals at the start of slot k. The second class of size $M - 2m - i$ nodes consists of those nodes in *BACK-OFF* state and their timers are not expired at the start of slot k plus those nodes in idle state with no arrivals at the start of slot k. The probability that a node from the first class is given as:

$$\lambda_1^k = p_{0,0,0,0}^k \beta + \sum_{i=1}^{C} \sum_{l=0}^{L} p_{i,0,l,0}^k \tag{31}$$

While the probability that a node from the second class is given as:

$$\lambda_2^k = p_{0,0,0,0}^k \bar{\beta} + \sum_{i=1}^{C} \sum_{l=1}^{L} \sum_{w=1}^{2^L} p_{i,0,l,w}^k \tag{32}$$

From (31) and (32), the probability $\Pr[S^k = l \mid \Psi^{k-1} = m]$ is given for $m = 0, 1, \cdots, \min\left(B-1, \left\lfloor\frac{M}{2}\right\rfloor\right)$ and $l = 0, 1, \cdots, M - 2m$ as follows:

$$\Pr\left[S^k = l \middle| \Psi^{k-1} = m\right] = C(M-2m, l)\left(\lambda_1^k\right)^l \left(\lambda_2^k\right)^{M-2m-l} \tag{33}$$

From equations (24), (26), (29), (30) and (33), the value of α^k in equation (23) is fully determined.

6 Performance metrics

In this section, we define the performance metrics used to evaluate the performance of the analysed protocol in terms of blocking probability, dropping probability, loss probability, queueing time, delay, the expected number of occupied bands, time to rendezvous (TTR) and throughput. All these calculations will be derived in steady-state. The blocking probability is defined as the probability that a packet arrives at a certain node finding its buffer is full. This probability is given as:

$$P_{block} = \sum_{j=0}^{1} \sum_{l=0}^{L} \sum_{w=0}^{2^l} p_{C,j,l,w}$$

A packet is dropped if a node reaches the maximum number of retransmission trails without winning the contention. In such case the dropping probability can be written as:

$$P_{drop} = \sum_{i=1}^{C} (1-\alpha) p_{i,0,L,0}$$

The loss probability P_{loss} is given as the summation of the blocking probability P_{block} due to those packets that are rejected and the dropping probability P_{drop} due to those packets that are pushed out due to the maximum number of retransmission is reached. Thus, P_{loss} can be expressed as follows.

$$P_{loss} = P_{block} + P_{drop}$$

The queueing time denoting the time of a packet inside the queue. This time starts from the arrival packet instant to its departing instant (either dropped or served). Using Little's formula, the queueing time Q is given as:

$$Q = \frac{\sum_{i=1}^{C} \sum_{j=0}^{1} \sum_{l=0}^{L} \sum_{w=1}^{2^l} ip_{i,j,l,w}^{k}}{\beta(1-P_{block})}$$

The delay time denoting the time of a packet inside the queue until gets served. This time starts from the arrival packet instant to its departing instant (i.e., served). Using Little's formula, the queueing time W is given as:

$$W = \frac{\sum_{i=1}^{C} \sum_{j=0}^{1} \sum_{l=0}^{L} \sum_{w=1}^{2^l} ip_{i,j,l,w}^{k}}{\beta(1-P_{block})(1-P_{drop})} + \frac{1}{s}$$

The TTR can be defined as the number of slots required by a sender and a receiver to arrive on the same data band to begin transferring data (Theis et al., 2011). As we mentioned above, a packet is dropped when it reaches the last backoff stage and experiences another collision. The average value of slots the station will utilise in the stage l, $l = 1, 2, \cdots, L$, is given by:

$$d_l = \frac{1+2+3+\cdots+2^l}{2^l}$$

The average number of slot times $E[R]$ required for a successful rendezvous can be found by multiplying the number of slots d_l the packet is delayed in each backoff stage $_l$ by the probability q_l that a packet is not dropped and reaches the l backoff stage:

$$E[R] = \sum_{l=0}^{L} d_l q_l$$

The probability q_l that a packet reaches the l backoff stage, provided that this packet is not to be discarded, is given as:

$$q_l = \frac{p_l - P_{drop}}{1 - P_{drop}}$$

where p_l is the probability that a node in stage l and given by:

$$p_l = \sum_{i=1}^{C} \sum_{w=1}^{2^l} p_{i,0,l,w}$$

The expected number of occupied bands $E[\Psi^k]$ is given as:

$$E[\Psi] = \sum_{j=1}^{\min\left(B-1, \left\lfloor \frac{M}{2} \right\rfloor\right)} j \Pr[\Psi = j]$$

Finally, the saturation throughput per node is given as follows. Since every packet that arrives and is not blocked and is not dropped must eventually be served, then:

$$Throughput = \frac{sE[\Psi]}{\beta(1-P_{block})(1-P_{drop})}$$

7 Simulation and discussion

7.1 Simulation setup

To validate the accuracy of the proposed Markov chain model, a discrete-event simulator using JAVA is developed to simulate UWB MAC protocol in basic access mode over a wide range of traffic loads and network sizes. The traffic at each node is generated using TCP model with geometric distribution. In other words, the packets arrive into nodes as a Bernoulli processes. The inter-arrival time is geometrically distributed with rate β. The value of β varying from 0.1 to s, where the service rate s is set to 0.9 in all simulation experiments. The scenario that we tested is organised as follows. The nodes are randomly distributed in an area of 500 × 500 m^2, where the number of nodes C is varying from 4 to 50 nodes. The *AODV* routing protocol is used to determine the path between senders and receivers. The buffer size at each node is set to 50 packets. The packet size is set to 1,024 bytes. When the queue is filled to its maximum capacity, the newly arriving packets are blocked until the queue has enough room to accept incoming traffic. When a nodes reaches its maximum retransmission, a packet is dropped from the head of the queue. The

simulation operational parameters values are listed in detail in Table 1.

Table 1 Operational parameters

Parameter	*Value*
Max. no. of collision, L	2, 4, 6
Transmission range	50 *m*
Packet size	1,024 Bytes
Routing protocol	AODV
Simulation time	10^6 *milliseconds*
Traffic load, β	Variable
Backoff time, w	*Random* $(1, 2^L)$

7.2 Performance evaluation

In this section, we use the same values of the buffer size C, the maximum number collisions L, the service time s and the values of arrival rate β as shown in Table 1 to generate numerical results for the measures obtained in Section (6). The system occupancy is calculated iteratively using Algorithm 1. In each iteration, the probability α that the *tagged sender* wins the contention on a valid receiver and a free band is computed until the steady-state is reached. Figure 4 plots blocking probability as a function of the traffic load. Moreover, different maximum number of collisions are generated, i.e., $L = 2$ and 4 to measure the effect of the maximum number of retransmission on the rejected packets. The figure shows that, the blocking probability increases with increasing the value of the traffic load for fixed buffer size $C = 50$ *packets*. On the other hand, increasing the value of L increases the blocking probability since as L increases the number of dropped packets decreases and hence the buffer is quickly fulfilled results in blocking of more packets. Figure 5 investigates the effect of the buffer size on the blocking probability. The figure shows that as the buffer size increases, the blocking probability decreases and hence the number of lost packets due to rejection is decreases.

Figure 4 The blocking probability versus the traffic load (see online version for colours)

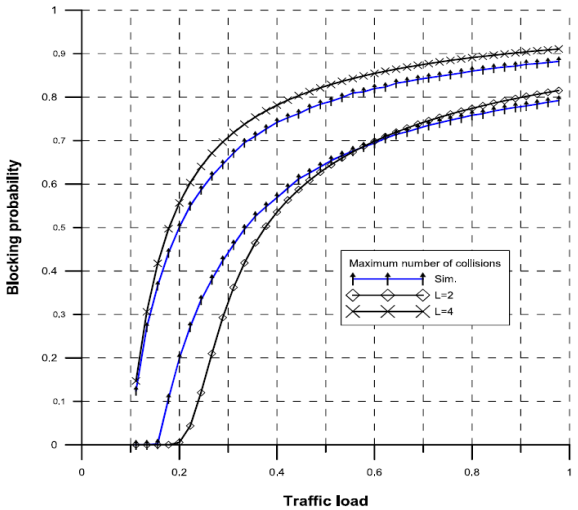

Figure 5 The blocking probability versus the traffic load and different buffer size

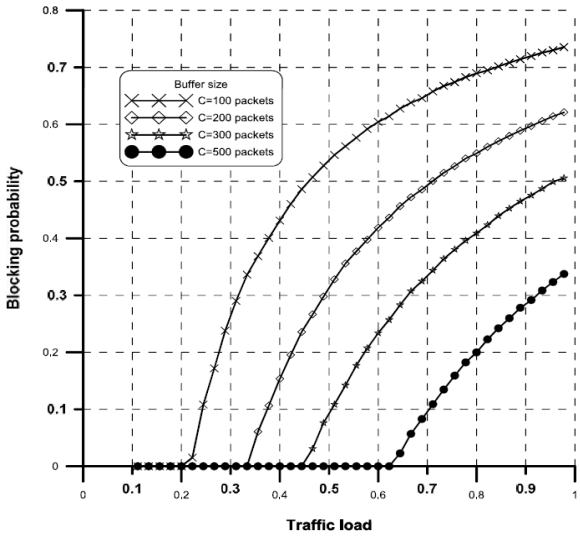

Figure 6 The drop probability versus the maximum number of collision (see online version for colours)

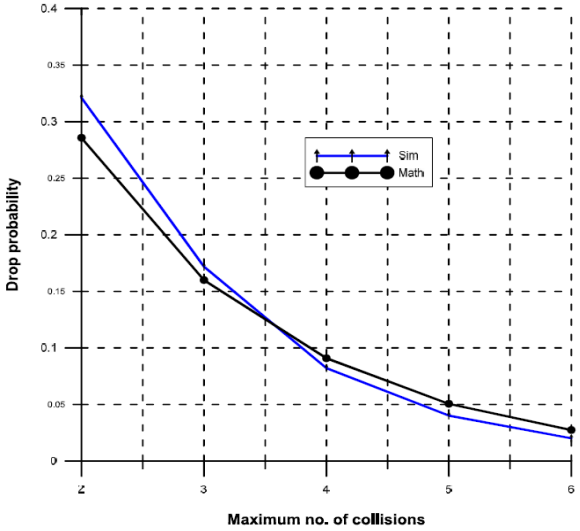

Figure 7 The drop probability versus the number of nodes (see online version for colours)

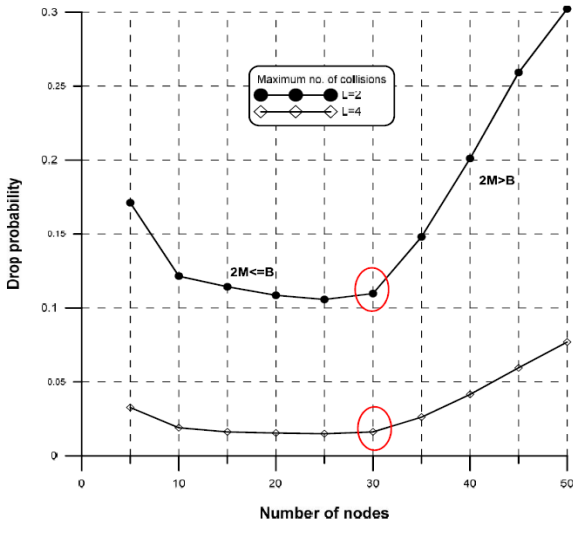

Figure 8 The average of queue length versus the traffic load (see online version for colours)

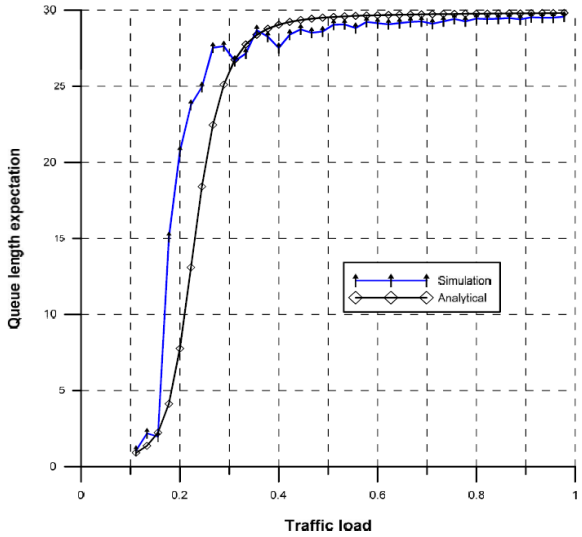

Figure 9 The average of queue delay versus the traffic load (see online version for colours)

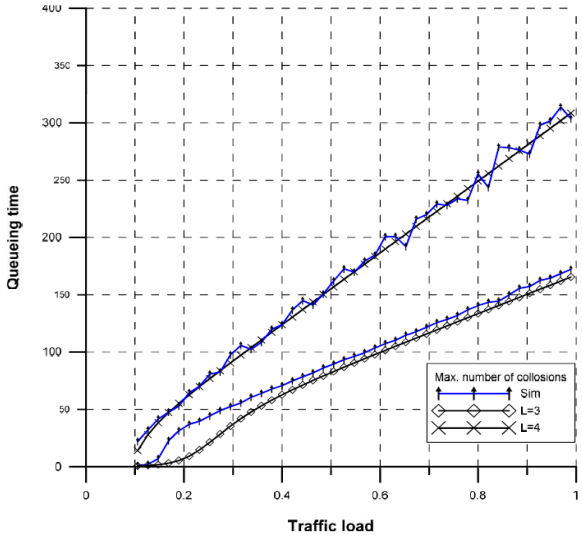

Figure 10 The band occupancy versus the number of nodes (see online version for colours)

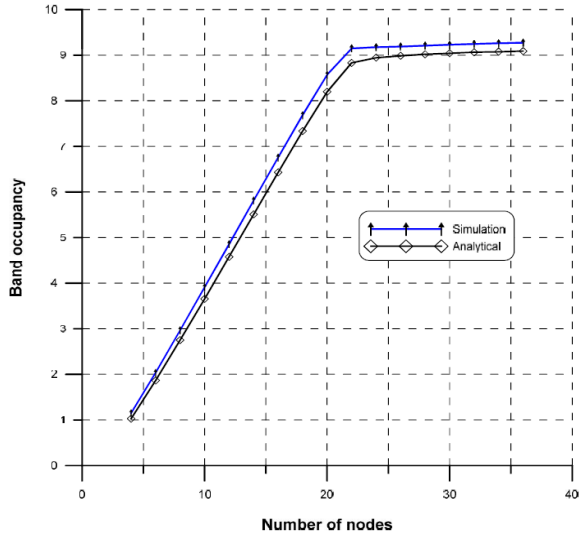

Figures 6–7 illustrate the effects of the maximum number of collisions L and the number of nodes M on the packets dropping probability. Figure 6 shows that for fixed number of nodes $M = 6$ and $B - 1 = 3$ (i.e., $M \leq 2\ (B - 1)$), the dropping probability decreases with increasing the value of L where the arrival rate $\beta = 0.5$ and the service rate $s = 0.9$. On the other hand, the adjustment of the initial contention window size $w = 2^L$ to higher values highly benefits packet drop probability. This means that, fewer packets are discarded since higher values of w reduces the number of collisions. Figure 7 shows that for $\left\lfloor \frac{M}{2} \right\rfloor \leq B-1$ the dropping probability decreases while for $\left\lfloor \frac{M}{2} \right\rfloor > B-1$ the dropping probability increases versus the number of nodes. This means that, for large network and small number of available bands the dropping probability increase. Figure 8 shows that higher values of traffic load cause an increase on queue length. Figure 9 plots packet queueing time versus the traffic load and for various maximum number of collisions. The figure shows that when the maximum number of collisions is small, more packets get served or dropped and hence the queueing time decreases. In this situation, the throughput improved if the number of dropped packets is less than the number of served packets. For large scale network, increasing or decreasing the maximum number of collision does not affect the queueing time. This observation is due to the random selection of receiver and band for the considered protocol. Figure 10 shows the average number of occupied bands as a function of the network size, M, for $L = 5$, $\beta = 0.5$, $s = 0.9$, the buffer size $C = 50$ and the number of available bands $B = 10$. The simulation results are very close to those computed mathematically for all the considered simulation experiments. From the figure we note that for large scale network, all the available bands are occupied all the time.

Figure 11 The throughput versus the number of nodes (see online version for colours)

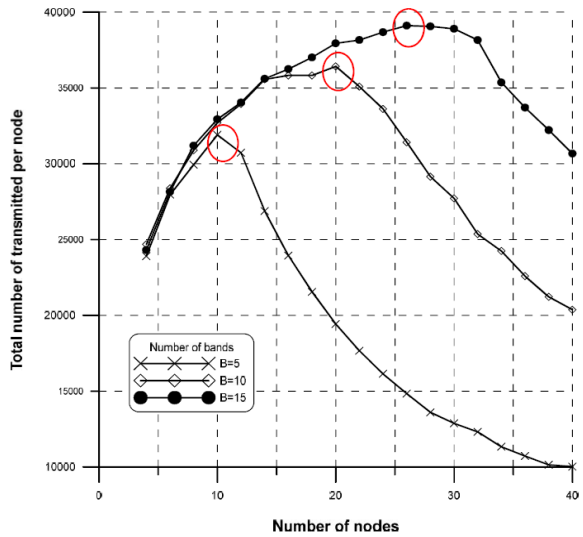

Figure 12 The throughput versus the traffic load (see online version for colours)

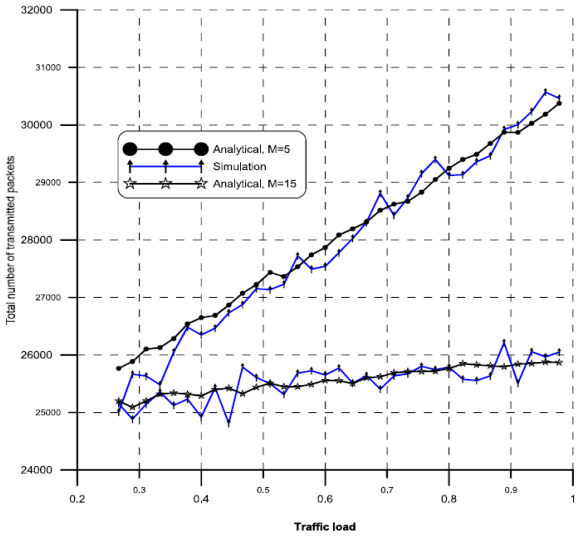

Figure 11 investigates the network throughput versus the network size under various number of available bands, the queue size C = 50 messages, β = 0.8 and s = 0.9. An interesting observation is that the throughput increases when $\left\lfloor \frac{M}{2} \right\rfloor \le B-1$. This observation is clear from the figure where at B = 10, the throughput increases until M = 20 after which it decreases. Clearly, for $\left\lfloor \frac{M}{2} \right\rfloor > B-1$ and regardless of queue length, the dropping probably increases due to the random receiver and band selection. Finally, Figure 12 illustrates the network throughput versus the traffic load under different network size given that $\left\lfloor \frac{M}{2} \right\rfloor \le B-1$, the queue size C = 50 messages, β = 0.8 and s = 0.9. From the figure, we observe that, regardless the number of bands B, when $\left\lfloor \frac{M}{2} \right\rfloor \le B-1$ the achieved throughput is better than the case when $\left\lfloor \frac{M}{2} \right\rfloor > B-1$.

7.3 Suggestions for collisions improvement

From performance metrics and the simulation results, we wish to point out here that, the considered protocol has many disadvantages like the collision and masked node problems that are raised due to the following events:

1 the busy receivers are not determined during the availability frame

2 the free bands are not preserved to one of the contending nodes during band's request stage

3 the requesting nodes are not known to each other

4 the collision probability increases with increasing the number of nodes even if the queue in not full

5 wasted capacity due to the use of control channel.

To improve the considered protocol, we may eliminate the availability frame and replace it with what we call the control frame. This can be implemented by dividing time into two parts. The first part is used to broadcast the control information to manage the traffic. Control information includes the status of the nodes and data bands. The other part of the time is used to transmit the data packets. The proposed structure of the control frame is as follows.

Table 2 Control frame's structure

Field	*Sender's IP*	*Priority*	*Status*	*Band*	*Receiver's IP*
Size in bits	8	8	2	6	8

According to the proposed frame structure shown in Table 2, all the previously stated problems are solved according to the following scenario. Each node (sender) sends (broadcasts) a control packet at its THS while a copy of this control packet is buffered in its buffer storage. All other nodes receive these packets during the other time differs from their THS. Since all nodes have the necessary information about the other nodes, they can know deterministically which the targeted receiver if more than one sender specify the same receiver. Also, each node can know deterministically which band can be used if more than one node request the same band. Nodes with high priorities always win contention. Initially, priorities are assigned to the node's IP host portion MOD N (32 or 64). If two nodes have the same, the node with the higher IP host portion wins the contention. IF flag = 0, then set the remaining fields to 0. Else, put the appropriate information.

We can describe the proposed improvement using the following scenario: let node A wants to start connection with node B on band B1 using B's THS. And node C wants to initiate a connection with node E using band B1 also during E's THS. Since both nodes B and E are free, they both replay with REQ_ACK on the band B1 at the same time which leads to collision. To overcome this problem, we force contending nodes to select the smaller band with respect to its IP. For example, let the contending nodes are N1, N2, N3, N4, N5 and N6 with IPs 192.168.1.1, 192.168.1.5, 192.168.1.7, 192.168.1.30, 192.168.1.221 and 192.168.1.123 respectively. Let the network address is given as 192.168.1.0. Let the available bands are B1, B 7, B10 and B11. Let N1 request N2, N3 request N5 and N4 request N6. According to our scheme, N1 has the smallest host portion (i.e., 1) among the others requesting nodes, therefore it will select B1. N3 has the second smallest host portion (i.e., 7) among the remaining others requesting nodes, therefore it will select B7. Note that N3 will never select B1 because it assumed that B1 is selected by N1 regardless whether B1 is actually selected or not. N4 has the third smallest host portion (i.e., 30) among the remaining others requesting nodes, therefore it will select B7. In future work, we aim to implement the proposed solution using both analytical and simulation approach and compare the result with the current considered protocol.

8 Conclusions

In this paper we evaluated the performance of a distributed multi-band MAC protocol utilises UWB technology to connect many devices in a WPAN. The work established an extensive analytical model based in queueing analysis of the buffers attached to the nodes. The work-based mainly on the work introduced in Broustis et al. (2007). However, we extend the work to involve queues in the analysis process, a new performance metrics are obtained. Also, a novel analytical approach is introduced.

According to the results obtained in the work, most of the results are expected. From the analysis it is shown that the optimal number of nodes to achieve good results is greater than or equal to twice the number of the available bands. However, after that number, the performance degrades dramatically. In all cases, the achieved throughput is better when the number of nodes is less twice the number of the available bands regardless of the number of bands.

The analysis shows a lot of drawbacks of the proposed protocol. Many suggestions can be taken in consideration to improve the proposed protocol and enhance its performance. Among our suggestions to improve the protocol is to eliminate collisions at receivers and bands by changing the negotiation method such that each sender knows in advance which nodes and bands are free.

Acknowledgements

This research was supported by Research Deanship, Hail University, KSA, on grant number 0150431.

References

Aripin, N.M., Fisal, N., Rashid, R. et al. (2009) 'Performance evaluation of video transmission over ultrawideband WPAN', in *Third Asia International Conference on Modelling & Simulation, AMS'09*, IEEE, pp.676–680.

Broustis, I., Krishnamurthy, S.V., Faloutsos, M., Molle, M. and Foerster, J.R. (2007) 'Multiband media access control in impulse-based UWB ad hoc networks', *IEEE Transactions on Mobile Computing*, Vol. 6, No. 4, pp.351–366.

Broustis, I., Vlavianos, A., Krishnamurthy, P. and Krishnamurthy, S.V. (2011) 'Mac layer throughput estimation in impulse-radio UWB networks', *IEEE Transactions on Mobile Computing*, Vol. 10, No. 5, pp.700–715.

Chen, H., Guo, Z., Yao, R.Y., Shen, X. and Li, Y. (2006) 'Performance analysis of delayed acknowledgment scheme in UWB-based high-rate WPAN', *IEEE Transactions on Vehicular Technology*, Vol. 55, No. 2, pp.606–621.

Gupta, A. and Mohapatra, P. (2007) 'A survey on ultra wide band medium access control schemes', *Computer Networks*, Vol. 51, No. 11, pp.2976–2993.

Han, M-S. (2013) 'Performance analysis of WiMedia UWB system with wireless video traffic', in *2013 15th International Conference on Advanced Communication Technology (ICACT)*, IEEE, pp.270–274.

Hu, C., Kim, H., Hou, J.C., Chi, D. and Shankar, N.S. (2010) 'A distributed approach of proportional bandwidth allocation for real-time services in ultrawideband (UWB) WPANS', *IEEE Transactions on Parallel and Distributed Systems*, Vol. 21, No. 11, pp.1626–1643.

Jiang, H. and Zhuang, W. (2007) 'Effective packet scheduling with fairness adaptation in ultra-wideband wireless networks', *IEEE Transactions on Wireless Communications*, Vol. 6, No. 2, pp.680–690.

Liu, K-H., Ling, X., Shen, X.S. and Mark, J.W. (2008) 'Performance analysis of prioritized MAC in UWB WPAN with bursty multimedia traffic', *IEEE Transactions on Vehicular Technology*, Vol. 57, No. 4, pp.2462–2473.

Liu, K-H., Shen, X., Zhang, R. and Cai, L. (2009) 'Performance analysis of distributed reservation protocol for UWB-based WPAN', *IEEE Transactions on Vehicular Technology*, Vol. 58, No. 2, pp.902–913.

Lu, K., Wu, D. and Fang, Y. (2005a) 'A novel framework for medium access control in ultra-wideband ad hoc networks', *Dynamics of Continuous, Discrete and Impulsive Systems (Series B) Special Issue on Ultra-Wideband (UWB) Wireless Communications for Short Range Communications*, Vol. 12, No. 3, pp.427–441.

Lu, K., Wu, D., Fang, Y. and Qiu, R.C. (2005b) 'On medium access control for high data rate ultra-wideband ad hoc networks', in *2005 IEEE Wireless Communications and Networking Conference*, IEEE, Vol. 2, pp.795–800.

Mohammed, M.S., Singh, M.J. and Abdullah, M. (2017) 'New TR-UWB receiver algorithm design to mitigate MUI in concurrent schemes', *Wireless Personal Communications*, Vol. 97, No. 3, pp.4431–4450.

Nassar, H. (1995) 'A Markov model for multi-bus multiprocessor systems under asynchronous operation', *Information Processing Letters*, Vol. 54, No. 1, pp.11–16.

Nassar, H. and Al Mahdi, H. (2003) 'Queueing analysis of an ATM multimedia multiplexer with non-pre-emptive priority', *IEE Proceedings-Communications*, Vol. 150, No. 3, pp.189–196.

Nassar, H. and Al-Mahdi, H. (2009) 'Design and analysis of a TDMA call assignment scheme for cellular networks', *Computer Communications*, Vol. 32, No. 7, pp.1200–1206.

Nassar, H. and Fouad, Y. (2003) 'Analysis of two-class discrete packet queues with homogenous arrival and prioritized service', *Communications in Information and Systems*, Vol. 3, No. 2, pp.101–117.

Ouanteur, C., Aïssani, D., Bouallouche-Medjkoune, L., Yazid, M. and Castel-Taleb, H. (2017a) 'Modeling and performance evaluation of the IEEE 802.15. 4e LLDN mechanism designed for industrial applications in WSNS', *Wireless Networks*, Vol. 23, No. 5, pp.1343–1358.

Ouanteur, C., Bouallouche-Medjkoune, L. and Aïssani, D. (2017b) 'An enhanced analytical model and performance evaluation of the IEEE 802.15. 4e TSCH CA', *Wireless Personal Communications*, Vol. 96, No. 1, pp.1355–1376.

Park, H., Lee, C., Lee, Y.S. and Kim, E-J. (2016) 'Performance analysis for contention adaptation of M2M devices with directional antennas', *The Journal of Supercomputing*, Vol. 72, No. 9, pp.3387–3408.

Rajamani, K., Soliman, S., Dural, Ö. and Rajkotia, A. (2008) 'Mac performance for second generation UWB', in *IEEE International Conference on Ultra-Wideband, ICUWB 2008*, IEEE, Vol. 1, pp.237–240.

Rosen, K.H. (1999) *Handbook of Discrete and Combinatorial Mathematics*, CRC Press, Boca Raton London New York Washington, DC.

Rosier, H., Frerichs, J. and Max, S. (2010) 'Interference aware scheduling for ultra wideband networks', in *2010 IEEE 6th International Conference on Wireless and Mobile Computing, Networking and Communications (WiMob)*, IEEE, pp.108–115.

Shen, X., Zhuang, W., Jiang, H. and Cai, J. (2005) 'Medium access control in ultra-wideband wireless networks', *IEEE Transactions on Vehicular Technology*, Vol. 54, No. 5, pp.1663–1677.

Theis, N.C., Thomas, R.W., DaSilva, L. et al. (2011) 'Rendezvous for cognitive radios', *IEEE Transactions on Mobile Computing*, Vol. 10, No. 2, pp.216–227.

Viswanathan, C. and Ravi, N. (2005) 'Mac protocol for UWB based ad hoc networks', in *2005 Annual IEEE INDICON*, IEEE, pp.64–67.

Zhejiang, H., Zhang, J-W. and Ying, Y. (2008) 'Multi-channel MAC protocol channel assignment based on location information of UWB ad hoc network', in *11th IEEE Internaational Conference on Communications Technology Proceedings*, IEEE, pp.122–112.

Zhuang, W., Shen, X. and Bi, Q. (2003) 'Ultra-wideband wireless communications', *Wireless Communications and Mobile Computing*, Vol. 3, No. 6, pp.663–685.

Zin, M.S.I.M. and Hope, M. (2010) 'A review of UWB MAC protocols', in *2010 Sixth Advanced International Conference on Telecommunications (AICT)*, IEEE, pp.526–534.